

See discussions, stats, and author profiles for this publication at: <https://www.researchgate.net/publication/228660369>

Texture entropy algorithm for automatic detection of oil spill from RADARSAT-1 SAR data

Article in *International journal of physical sciences* · September 2010

CITATIONS

20

READS

174

2 authors, including:



Mazlan Hashim

Universiti Teknologi Malaysia

356 PUBLICATIONS 2,303 CITATIONS

SEE PROFILE

Some of the authors of this publication are also working on these related projects:



Spectral Characterisation of Triggering Biophysical Properties of General Flowering using Satellite Remote Sensing Data [View project](#)



mesoscale eddies [View project](#)

Full Length Research Paper

Texture entropy algorithm for automatic detection of oil spill from RADARSAT-1 SAR data

Maged Marghany* and Mazlan Hashim

Institute of Geospatial Science and Technology (INSTEG), Universiti Teknologi Malaysia 81310 UTM, Skudai, JohoreBahru, Malaysia.

Accepted 12 August, 2010

This work presents a method based on the utilisation of texture algorithms for the discrimination of oil spill areas from the surrounding features, e.g. sea surface and look-alikes, using RADARSAT-1 SAR Wide beam mode (W1), Standard beam mode (S2) and Standard beam mode (S1) data acquisition under different wind speeds. The results show that entropy texture algorithm is able to discriminate between oil spills and look-alike areas. The results also illustrate that the entropy texture algorithm identifies well the deficiency of oil spills in pairs of S2 data. Further, the W1 mode data, however, show an error standard deviation of 0.002, thus performing a better discrimination of oil spills than the S1 and S2 mode data.

Key words: RADARSAT-1 SAR, W1 mode, S2 mode, oil spill, entropy texture algorithm.

INTRODUCTION

Synthetic aperture radar (SAR) has been recognised as a powerful tool for oil spill detection. SAR data have unique features as compared to optical satellite sensors which makes the satellite particularly valuable for spill monitoring. These features are involved with several parameters: operating frequency, band resolution, incidence angle and polarisation. For instance, RADARSAT-1 SAR data have an operating frequency of 5.3 GHz with HH polarisation, in which the radar backscatter from sea surface at large tilt modulation can be measured. Consequently, the width of the observed swath depends on the imaging mode, varying from 50 to 500 km, with nominal resolutions of 10 - 100 m. In practice, RADARSAT-1 SAR data have various beam incidence angles for the seven standard imaging modes, which range from 20 to 49° off vertical. The extended low and high-incidence modes, nevertheless, provide access to incidence angles from 10 to 59°. Although the image is usually re-sampled to a uniform pixel resolution of 12.5 m across the swath, the nominal resolution of the sensor in standard mode is 25 m. Further, a dark oil spill spot on the ocean can be viewed every 1 to 3 days by virtue of

the variable RADARSAT-1 SAR beam modes and their variable incidence angles, which are considered the most advantageous parameters of RADARSAT-1 SAR data (Solberg and Volden, 1997; Maged et al., 2009b).

Several algorithms have been introduced for the automatic detection of oil spills in SAR images. These algorithms have involved three steps: (i) dark spot detection, (ii) dark spot feature extraction and (iii) dark spot classifications. Various classification of algorithms for oil spill detection have been utilized, including pattern recognition algorithms (Fukunaga, 1990), spatial frequency spectrum gradient (Lombardini et al., 1989; Trivero et al., 1998) and fuzzy and neural networks techniques (Mohamed et al., 1999; Calabresi et al., 1999). This step is controlled by wind conditions and the type of SAR sensors. In general, the sea surface appears dark in SAR images when the wind speeds are ranged between 0 and 2.3 m/s.

Therefore, the oil spill detections under the low wind speeds are probable. In fact, the wind-generated waves are not already developed and oil spill looks like a dark spot in SAR image. According to Solberg and Volden (1997), the ideal detection of oil spill in SAR images requires a moderate wind speed which should not exceed 6 m/s. Nevertheless, in regions of higher wind speed of 10 - 12 m/s, slick disappears from the sea surface and

*Corresponding author. E-mail: magedupm@hotmail.com.

Table 1. RADARSAT-1 SAR Wide (W1), Standard (S2) and Standard (S1) characteristics were used in this study.

Beam mode	Incidence angle (°)	Swath area (km)	Looks	Width (km)	Resolution (Range × Azimuth, m)
W1	20 - 31	150	4	165	30 - 48 × 28
S2	23.7 - 31	100	3.1	100	25 × 28
S1	23.7 - 31	100	3.1	100	25 × 28

SAR imagery due to the redistribution of oil slicks by the surface waves and wind-induced mixing in the upper ocean layer.

A new approach has been introduced by Maged (2001) to detect thin and linear slicks by using the Lee algorithm (Touzi, 2002). The Lee Filter is primarily used on radar data to remove high frequency speckles without removing edges or sharp features in the images. Maged and van Genderen (2001) reported that the Lee algorithm operates well to determine linear slick features. According to Maged (2001) the Lee algorithm avoids decreasing resolution by making a weighted combination of running average which reduced the noise in the slick's edge areas without sacrificing edge sharpness.

Furthermore, Maged and van Genderen (2001) introduced a new approach by using texture algorithms for automatic detection of oil spills in a RADARSAT-1 SAR image. In fact, grey-tone spatial-dependence or co-occurrence matrices provide the basis for a number of measures including range, variance, standard deviation, entropy, or uniformity within a moving kernel window. However, computing the texture features from a co-occurrence matrix may become critical due to the multiplicative noise impacts.

Recently, Shi et al. (2008) used entropy texture algorithm for oil spill detection from ENVISAT and MODIS satellite data. They found that the oil spill pixels are smoother than the surrounding environment. In fact, texture entropy algorithm has removed the speckle from oil spill pixels in SAR data.

Further, Akkartal and Sunar (2008) used entropy algorithm with thresholding and segmentation techniques for oil spill detection from RADARSAT-1 SAR data. They reported that high contrasted areas representing oil spill, have more homogeneity, less entropy and more second angular moment values regarding to its background.

This work has hypothesized that the dark spot areas (oil slick or look-alike pixels) and its surrounding back-scattered environmental signals in the SAR data can be modeled as texture. In this context, a co-occurrence texture algorithm entropy can be used as a semi-automatic tool to discriminate between oil spills, look-alikes and surrounding sea surface waters. In doing so, this study has extended the previous work done by Maged (2001) and Maged and Genderen (2001) who used the RADARSAT-1 SAR different beam mode data that is, wide beam mode (W1) and standard beam mode (S2) to illustrate the extended theory.

RESEARCH METHODS

Data set

The SAR data acquired in this study was from the RADARSAT-1 Wide beam mode (W1), Standard beam mode (S2) and (S1) images, respectively. These data are C-band and have a lower signal-to noise ratio due to their HH polarization with wavelength of 5.6 cm and frequency of 5.3 GHz. RADARSAT-1 wide beam mode (W1) data have four independent looks and cover incidence angles of 20 to 31° (Maged et al., 2009a) while the Standard beam mode (S2) and (S1) data have 3.1 looks and cover incidence angle of 23.7 and 31.0° (Maged et al., 2009b). Indeed, spatial averaging of (4-look) SAR data reduces signal level fluctuation due to speckle to about 5% which is equivalent to 0.2 dB.

Therefore, a calibration accuracy of 0.2 dB appears an appropriate task for slick detection in RADARSAT-1 data. In addition, Wide beam mode (W1) data and Standard beam mode (S2) cover the swath width of 165 and 100 km, respectively. Furthermore, both data have different azimuth resolution and a ground range resolution (Table 1). Both Mohamed et al. (1999) and Samad and Shattri (2002) reported that the occurrence of oil spill pollution on 15 December, 1997 and 20 December, 1999, respectively along the coastal water of the Malacca straits. Further, it was observed that several oil spill parcels along the east coast of Mersing, Johor, Malaysia during the physical ocean parameter collections on 26 March, 2008 (Maged et al., 2009b).

Texture algorithm

Co-occurrence is applied to categorize the image to "oil slick" and water. Entropy texture with 0° angular relationship and $d = 1$ is employed. On the other hand, RADARSAT-1 SAR gray tone can be described as texture (that is, the microstructure). A co-occurrence matrix or co-occurrence distribution (less often co-occurrence matrix or co-occurrence distribution) is a matrix or distribution that is defined over an image to be the distribution of co-occurring values at a given offset. Mathematically, a co-occurrence matrix C is defined over an $n \times m$ image I , parameterized by an offset $(\Delta x, \Delta y)$, as:

$$C_{\Delta x, \Delta y}(i, j) = \sum_{p=1}^n \sum_{q=1}^m \begin{cases} 1, & \text{if } I(p, q) = i \text{ and } I(p + \Delta x, q + \Delta y) = j \\ 0, & \text{otherwise} \end{cases} \quad (1)$$

According to Maged (2001) the texture feature for oil spill and look-alike detections are computed by the following formula:

$$Ent = \sum \sum p_{ij} \log p_{ij} \quad (2)$$

Where Ent is Entropy, i and j are the row and column, p_{xi} and p_{yj} are the marginal probability matrix obtained through the summation of p_{ij} in the direction of the row and column.

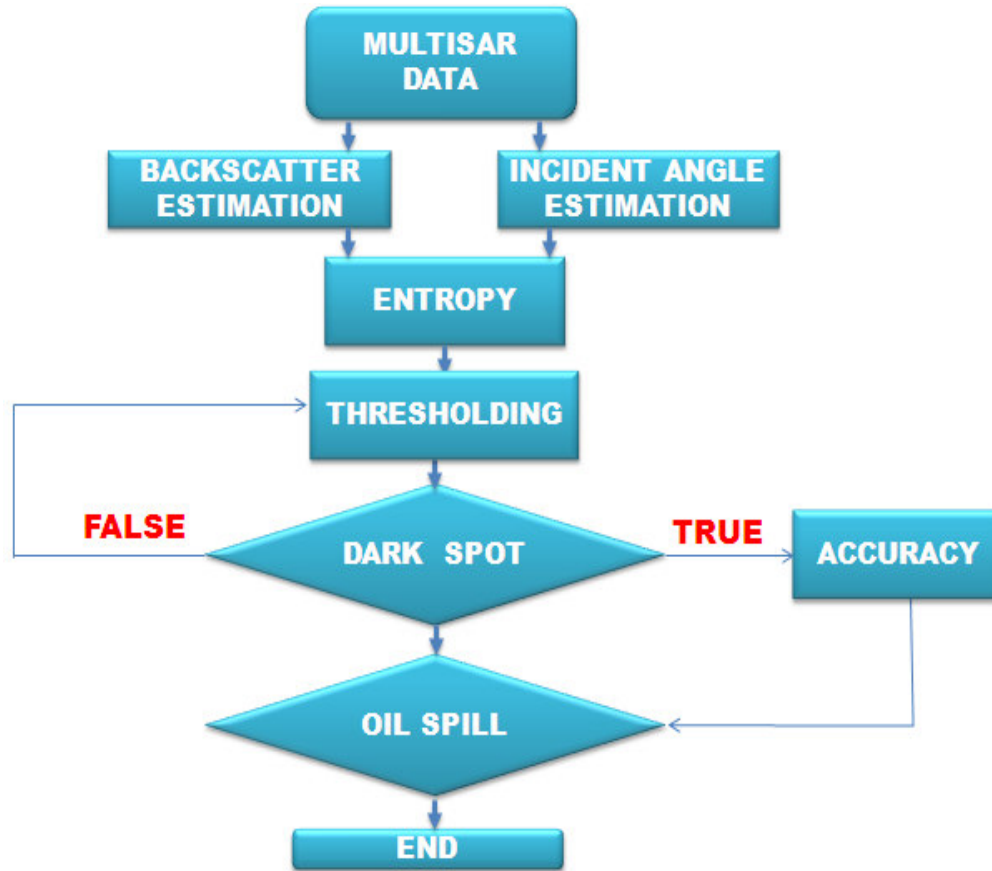


Figure 1. Block diagram of oil spill detection.

The procedures of entropy algorithm implementation to multiSAR data are shown in Figure 1. In this study, the window size is 7×7 pixels and lines (Maged, 2001). According to Maged (2001) the window size of 7×7 gives more details on an image. Window size is used for producing the co-occurrence matrix for each input pixel.

RESULTS AND DISCUSSION

The co-occurrence texture algorithms are trained on 3 different RADARSAT-1 SAR mode data, whereas the dark spots are identified and examined. The RADARSAT-1 SAR images contain the confirmed oil spills which occurred near the west and east coasts of Peninsular Malaysia on 26 December, 1997 (Mohamed et al. 1999), 20 December, 1999 (Samad and Shattri, 2002), and 26 March, 2008, respectively (Figure 2). Further, *in situ* observations have confirmed the occurrence of oil spills on 26 March, 2008 along the coastal water of Mersing, Johor, Malaysia.

Figure 3 shows the variation of the average backscatter intensity along the azimuth direction in the oil-covered areas as function of incidence angles for the W1, S2 and S1 modes, respectively. The backscattered intensity is damped by -8 to -18 dB in W1, -10 to -18 dB in S2 and

-11 to -18 dB in S1 mode data (Figure 3). Further, three different mode backscatter intensities are above the RADARSAT-1 noise floor value of nominally -20 dB. In fact RADARSAT-1 SAR is a C-band instrument with a variable acquisition swath, presenting large variety of possible incidence angles, swath widths, and resolutions (Maged et al., 2009a). It is argued that oil slicks can be detected with a contrast as small as 4 dB. This suggests that a large part of the RADARSAT-1 swath could be useful for oil slick detection. Nevertheless, Ivanov et al. (2002) reported that the RADARSAT-1 SAR, in its ScanSAR Narrow mode with swath width that exceeds 300 km, is an attractive tool for marine oil pollution detection.

Clearly, Figure 4 shows that the entropy algorithm isolates the oil spill from its surrounding pixels in three different RADARSAT-1 SAR mode data. In fact, entropy used to separate between oil spill pixels, sea water and land. According to Maged (2001), entropy is measure of uniformity in SAR image. In general, the entropy is a measure of variability or randomness because the concentration of the backscatter changes in relatively few locations would be non-random essentially. In other words, entropy measures the absolute variability in

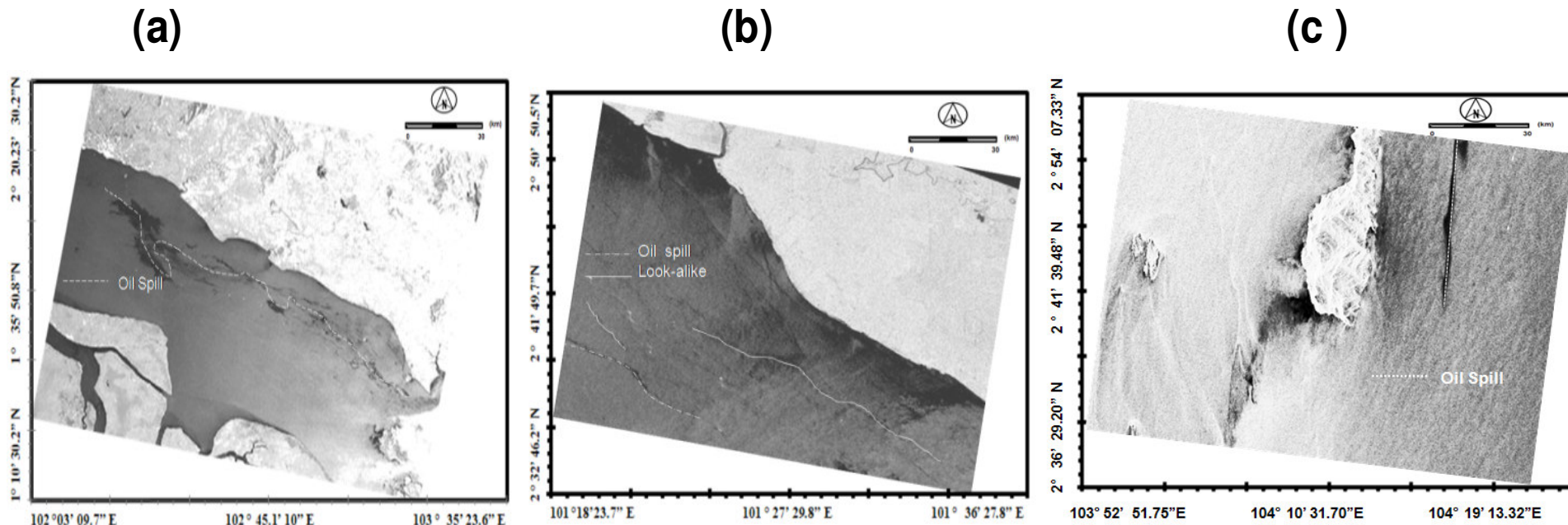


Figure 2. Oil spill locations are indicated by dash lines during acquisition of (a) RADARSAT-1 Wide mode (W1), (b) RADARSAT-1 Standard mode (S2) and (c) RADARSAT-1 SAR Standard mode (S1).

in backscatter change over the selected window. For oil spill detection, the lowest error standard deviation of 0.002 occurs in W1 mode data (Figure 5). This means that W1 performs better detection for oil spill as compared to S1 and S2 mode data. In fact, W1 shows steeper incident angle of 30° than both S1 and S2 mode data. In addition, the offshore wind speed during W1 overpass was 4.11 m/s while the offshore wind speed was 7 m/s during S2 overpass. In fact, wind speeds which do not exceed 6 m/s are appropriate for ideal detection of oil spill in SAR data (Solberg and Volden, 1997). Therefore, for application that require imaging of the ocean surface, steep incidence angles are preferable due to a greater contrast of backscatter which are

manifested at the ocean surface. This confirms the study of Maged et al. (2009b). Previous studies were concerned with automatic detection of oil spills from SAR images, which is based on dark spot feature extraction and classification (Solberg and Solberg, 1997; Solberg and Volden, 1997; Benelli and Garzelli 1999; Mohamed et al., 1999; Samad and Shattri, 2002; Maged and Genderen, 2001). In contrast to the present study, those studies failed to isolate the oil spill from surrounding environment pixels by using different segmentation algorithms (Solberg and Volden, 1997; Mohamed et al., 1999; Samad and Shattri, 2002). Indeed, the different oil spill segmentation approaches, in terms of accuracy of classification of oil spills and features of the

surrounding sea, are a challenging task; the modification of the algorithms used for automatic detection of oil spills might be required to improve the analyses.

Conclusion

This aim of this study is to compare between RADARSAT-1 SAR different mode data of Wide beam mode (W1), Standard beam mode (S2) and Standard beam mode (S1) data acquisition under different wind speeds for oil spill detection. In doing so, the texture co-occurrence algorithm of entropy has applied kernel window size of 7 × 7 pixels and lines. The results show that entropy

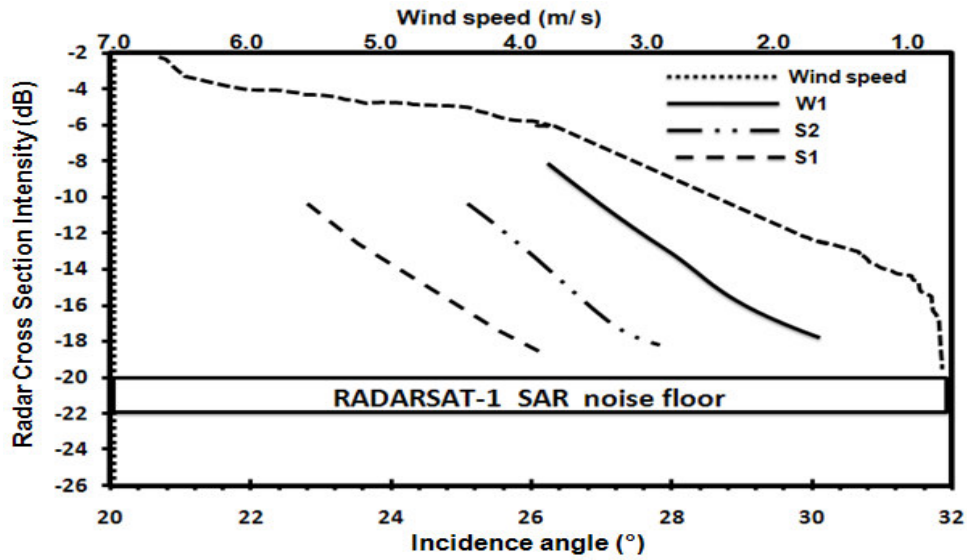


Figure 3. Radar cross section intensity along oil slick locations in W1, S1 and S2 and wind speed distribution during date of acquisitions.



Figure 4. Oil spill detection using entropy algorithm with kernel window size 7×7 pixels and lines in W1, S1 and S2 mode data.

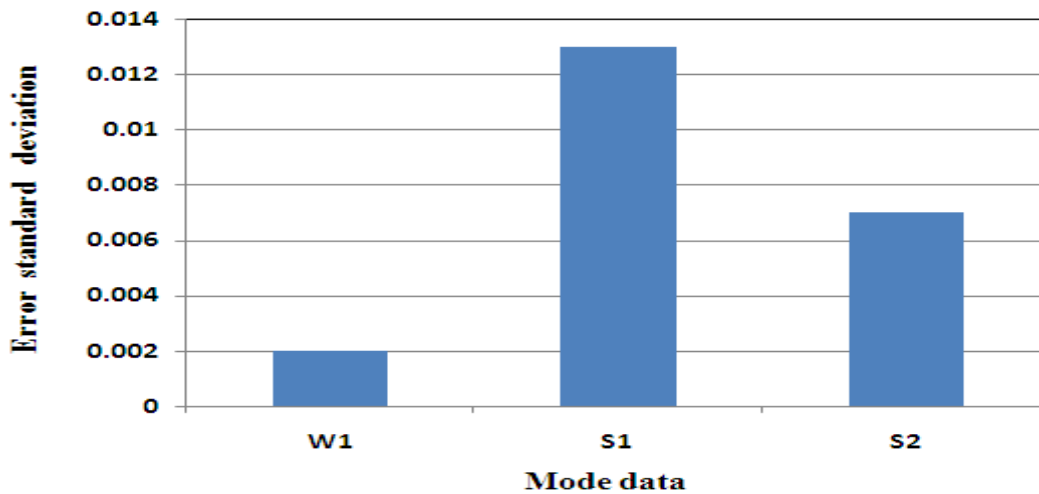


Figure 5. Error standard deviation of different RADARSAT-1 SAR mode data.

texture algorithm has excellent discrimination between oil spills and look-alike areas. In addition, the W1 mode data, however, show an error standard deviation of 0.002, thus performing a better discrimination of oil spills than the S1 and S2 mode data. Entropy can be used as automatic tool for oil spill in different RADARSAT-1 SAR different mode data under dissimilar wind speed patterns.

REFERENCES

- Akkartal A, Sunar F (2008). The usage of radar images in oil spill detection. http://www.isprs.org/proceedings/XXXVII/congress/8_pdf/2_WG-VIII-2/16.pdf.
- Calabresi G, Del Frate F, Lightenegger J, Petrocchi A, Trivero P (1999). Neural networks for the oil spill detection using ERS-SAR data. In Proceedings of Geoscience and Remote Sensing Symposium, IGARSS'99, Hamburg, Germany, 28 June-2 July, IEEE Geosci. Remote Sensing Society, USA, 1: 215-217.
- Fukunaga K (1990). Introduction to statistical pattern recognition. 2nd edition, Academic Press, New York.
- Lombardini PP, Fiscella B, Trivero P, Cappa C, Garrett WD (1989). Modulation of the spectra of short gravity waves by sea surface films: slick detection and characterization with microwave probe. J. Atmospheric Oceanic Technol., 6: 882-890.
- Ivanov A, He M, Fang MQ (2002). Oil spill detection with the RADARSAT SAR in the waters of the Yellow and East Sea: A case study CD of 23rd Asian Conference on Remote Sensing, 13-17 November, Nepal, Asian Remote Sensing Society, Japan, 1: 1-8.
- Maged M (2001). RADARSAT automatic algorithms for detecting coastal oil spill pollution. Int. J. Appl. Earth Observation Geoinformation, 3: 191-196.
- Maged M, vanGenderen J (2001). Texture algorithms for oil pollution detection and tidal current effects on oil spill spreading. Asian J. Geoinformatics, 1: 33-44.
- Maged M, Cracknell A, Mazlan H (2009a). Modification of Fractal Algorithm for Oil Spill detection from RADARSAT-1 SAR data. Int. J. Appl. Earth Observation Geoinformation, 11: 96-102.
- Maged M, Cracknell A, Mazlan H (2009b). Comparison between radarsat-1 SAR different data modes for oil spill detection by a fractal box counting algorithm. Int. J. Digital Earth, 2(3): 237-256.
- Mohamed IS, Salleh AM, Tze LC (1999). Detection of oil spills in Malaysian waters from RADARSAT Synthetic Aperture Radar data and prediction of oil spill movement. Proceeding of 19th Asian Conference on Remote Sensing, China, Hong Kong, 23- 27 November, Asian Remote Sensing Society, Japan, 2: 980-987.
- Samad R, Mansor SB (2002). Detection of Oil spill Pollution using RADARSAT SAR Imagery. Proceedings of 23rd Asian Conference on Remote Sensing, Birendra International Convention Centre in Kathmandu, Nepal, November 25 - 29, Asian Remote Sensing Society, Nepal. <http://www.gisdevelopment.net/acrs/2002/sar/096.pdf>.
- Shi LZ, Fan C, Shi K, Peng L (2008). Texture feature application in oil spill detection by satellite data. Proceedings of Image and Signal Processing, CISP, Sanya, China, 27-30 May, pp. 784-788.
- Solberg AHS, Volden E (1997). Incorporation of prior knowledge in automatic classification of oil spills in ERS SAR images. In International Geoscience and Remote Sensing Symposium, pp. 3-8. Aug., Singapore, IEEE Geosci. Remote Sensing Society, USA, 1: 157-159.
- Trivero P, Fiscella B, Gomez F, Pavese P (1998). SAR detection and characterization of sea surface slicks. Int. J. Remote Sensing, 19: 543-548.
- Touzi R (2002). A review of speckle filtering in the context of estimation theory, IEEE Trans. Geosci. Remote Sensing, 40: 2392-2404.